The Journal of Neuroscience, July 15, 1996, 16(14):4376–4382

Functional Correlation of NMDA Receptor ε Subunits Expression with the Properties of Single-Channel and Synaptic Currents in the Developing Cerebellum

Tomoyuki Takahashi,[1] Dirk Feldmeyer,[4] Norimitsu Suzuki,[1] Kayoko Onodera,[1] Stuart G. Cull-Candy,[4] Kenji Sakimura,[3] and Masayoshi Mishina[2]

[1]Department of Neurophysiology, Institute for Brain Research and [2]Department of Pharmacology, Faculty of Medicine, University of Tokyo, 113 Tokyo, Japan, [3]Department of Neuropharmacology, Brain Research Institute, Niigata University, Niigata 951, Japan, and [4]Department of Pharmacology, University College London, London WC1E 6BT, United Kingdom

NMDA receptor (NMDAR) subunits ε1–ε4 are expressed differentially with respect to brain region and ontogenic period, but their functional roles still are unclear. We have compared an ε1 subunit-ablated mutant mouse with the wild-type to characterize the effect of ε subunit expression on NMDAR-mediated single-channel currents and synaptic currents of granule cells in cerebellar slices. Single-channel and Western blot analyses indicated that the ε2 subunit disappeared gradually during the first postnatal month in both wild-type and mutant mice. Concomitantly, the voltage-dependent Mg^{2+} block of NMDAR-mediated EPSCs (NMDA-EPSCs) was decreased. Throughout the developmental period studied, postnatal day 7–24 (P7–P24), the decay time course of NMDA-EPSCs in ε1 mutant (−/−) mice was slower than in wild-type mice. We suggest that the expression of the ε3 subunit late in development is responsible for a reduction in the sensitivity of NMDA-EPSCs to block by extracellular Mg^{2+} and that receptors containing the ε1 subunit determine the fast kinetics of the NMDA-EPSCs.

Key words: NMDA receptor; synaptic current; single channel; cerebellum; gene targeting; patch clamp

In the cerebellum, NMDA receptors (NMDARs) are thought to play important roles in neuronal development (Rabacchi et al., 1992; Komuro and Rakic, 1993) and excitatory synaptic transmission (Garthwaite and Brodbelt, 1989; Silver et al., 1992; D'Angelo et al., 1993). Molecular cloning studies have revealed five NMDAR subunits called ζ1 and ε1–ε4 in mice (Ikeda et al., 1992; Kutsuwada et al., 1992; Meguro et al., 1992; Yamazaki et al., 1992) or NR1 and NR2A–NR2D in rats (Moriyoshi et al., 1991; Monyer et al., 1992). The ζ1 (NR1) subunit is indispensable for channel function (Moriyoshi et al., 1991), and its mRNA is expressed ubiquitously, whereas the ε (NR2) subunit mRNAs are expressed differentially with respect to cerebellar region and age (Watanabe et al., 1992, 1994; Akazawa et al., 1994; Monyer et al., 1994). In cerebellar granule cells, ε2 subunit mRNA is expressed transiently during early postnatal development, whereas ε1 and ε3 subunit mRNAs are expressed at a relatively late stage (Watanabe et al., 1992; Akazawa et al., 1994; Monyer et al., 1994). Recombinant NMDARs composed of the ζ1 (NR1) subunit and one of the ε (NR2) subunits show distinct characteristics according to the type of ε subunits involved. The ε subunit-dependent properties include single-channel conductance and kinetics (Stern et al., 1992; Tsuzuki et al., 1994), time course of current deactivation (Monyer et al., 1992, 1994), affinity for agonists, sensitivity to antagonists (Kutsuwada et al., 1992; Ishii et al., 1993), glycine, phorbol ester (Kutsuwada et al., 1992), and Mg^{2+} (Kutsuwada et al., 1992; Monyer et al., 1992, 1994; Ishii et al., 1993). To study whether these ε subunit-dependent characteristics are reflected in native NMDARs, we have recorded NMDAR-mediated single-channel currents and synaptic currents from granule cells in cerebellar slices. To enable the role of each ε subunit to be determined in isolation, we have used mutant mice with their ε1 subunit ablated by gene knock-out techniques (Sakimura et al., 1995) and compared the single-channel and synaptic currents in wild-type and mutant mice at early and late postnatal periods. The results from these experiments indicate that both ε1- and ε3-containing receptors can be present at the synapse. Expression of the ε1 subunits result in a relatively fast decay of the NMDAR-mediated EPSCs (NMDA-EPSCs), whereas late expression of the ε3 subunits contributes to a developmental reduction in the voltage-dependent block of the EPSC by Mg^{2+}.

MATERIALS AND METHODS

Preparation and solutions. Wild-type and ε1 subunit-ablated mutant mice were decapitated with scissors under ether anesthesia. After isolating the cerebellum, parasagittal slices were cut using a tissue slicer (DTK 1000, Dosaka). Slice thickness was 150–200 μm for single-channel recordings and 250–300 μm for recording synaptic currents. Slices were incubated at 36.5°C for 1 hr in a submerged chamber or left at room temperature in a moist chamber equilibrated with 95% O_2/5% CO_2. For experiments, slices were transferred into a superfusing chamber on a stage of upright microscope (Axioskop, Zeiss, Jena, Germany), and cells were viewed under Nomarski optics. Standard superfusate had the following composition (in mM): NaCl 125; KCl 2.5; NaH_2PO_4 1.26; $NaHCO_3$ 26; glucose 15; $CaCl_2$ 2; $MgCl_2$ 1.0, pH 7.4, when bubbled with 95% O_2/5% CO_2. In some experiments, $MgCl_2$ in the superfusates was reduced to 0 mM or 0.1 mM. The superfusate routinely contained bicuculline (10 μM) (Sigma, St. Louis, MO), strychnine (0.5–1.0 μM) (Sigma), and glycine (10 μM) (Wako, Japan). CNQX (20 μM) (Tocris Cookson, Bristol, UK) was added to the superfusate to isolate the NMDAR-mediated component from the

Received Feb. 26, 1996; revised April 26, 1996; accepted May 1, 1996.

This work was supported by the Monbusho International Scientific Research Program of Japan (T.T.) and by the Wellcome Trust and the Howard Hughes Medical Institute (S.G.C.C.). We are grateful to Drs. Mark Farrant, Toshiya Manabe, and Yasunori Hayashi for critical reading of this manuscript, and Drs. David Colquhoun and Stephen Traynelis for generously providing software.

Correspondence should be addressed to Tomoyuki Takahashi, Department of Neurophysiology, Institute for Brain Research, Faculty of Medicine, University of Tokyo, Tokyo 113, Japan.

Dr. Feldmeyer's present address: Abteilung für Zellphysiologie, Max-Planck-Institute für Medizinische Forschung, D-69120 Heidelberg, Germany.

 0270-6474/96/164376-07$05.00/0

AMPA receptor-mediated component of EPSCs. Patch pipettes were pulled from borosilicate glass (Clark GC150F-7.5), coated with Sylgard resin, and fire-polished to a final resistance of 5–10 MΩ for whole-cell recording or 15–20 MΩ for excised patch recordings. The pipette solutions contained (in mM): Cs gluconate 110; CsCl 30; NaCl 4; HEPES 10; EGTA 5; $CaCl_2$ 0.5, adjusted to pH 7.3 with CsOH. The pipette solution for recording synaptic currents also contained 2 mM MgATP to protect NMDARs from run down and 5 mM *N*-(2,6-dimethylphenylcarbamoylmethyl)-triethyl-ammonium bromide (QX314) (Research Biochemicals, Natick, MA) to suppress action potentials.

Single-channel and whole-cell recordings from cerebellar granule cells. Single-channel and whole-cell current recordings were made from cells in the internal granule cell layers using an EPC-7 (List) amplifier. The cell capacitance was measured from the amplifier, and cells with a capacitance less than 5 pF were regarded as granule cells. The mean input resistance of granule cells was 2.95 ± 0.24 GΩ (± SEM, $n = 11$). Single-channel recordings were made from outside-out patches excised from visually identified granule cells (Edwards et al., 1989; Farrant et al., 1994). NMDA (50 μM) (Sigma) was bath applied to a patch by switching the superfusion line. Whole-cell recordings of EPSCs were made primarily using the blind techniques (Blanton et al., 1989). The mean access resistance with this method was 67.5 ± 4.9 MΩ ($n = 11$) corresponding to 2.3% of granule cell access resistance. Given the relatively slow time course of NMDA-EPSCs, kinetic distortion by the access resistance was negligible. EPSCs were evoked by stimulating mossy fibers at 0.1 Hz at the white matter with a patch pipette (tip diameter, 3–5 μm) filled with 1 M NaCl. In earlier experiments on Mg^{2+} block, NMDA-EPSCs also were recorded from visually identified granule cells. Results obtained by the two methods were essentially the same; therefore, the data were pooled. All experiments were performed at room temperature (23–26°C).

Single-channel and whole-cell current analyses. Single-channel currents were stored using a tape recorder (BioLogic DTR-1204) (bandwidth DC to 5.0 kHz) and analyzed off line. Records were filtered with an eight-pole Bessel filter at a cut-off frequency of 2 kHz (−3 dB) and digitized at 20 kHz (PC-AT personal computer equipped with a CED 1401+ interface). Patches with high noise levels were excluded from analysis to avoid ambiguities in channel identification. Amplitudes of single-channel events were determined by the method of time course fitting (Colquhoun and Sigworth, 1995). Mean single-channel currents were obtained from maximum likelihood fits of the sum of 2–4 Gaussian distributions to the cursor fitted amplitudes (Colquhoun and Sigworth, 1995). Only events longer than two filter rise times (332 μsec) were included in the amplitude distributions, i.e., openings that had reached at least 99% of their full amplitude to avoid the problem of assigning openings to wrong conductance levels. Single-channel chord conductances were calculated on assuming a reversal potential of 0 mV (Farrant et al., 1994). NMDA-EPSCs were low-pass filtered at 0.5 kHz, digitized at 2.5 kHz (Dagan LM-12S interface), and analyzed on a personal computer (Dell 466/LV). Holding potentials were not corrected for the liquid junction potential between pipette solution and superfusate (+7 mV). All values are expressed as mean ± SEM.

Measurement of the ε1 and ε2 subunit proteins. Rabbit anti-ε1 and anti-ε2 antibodies were raised against fusion proteins containing a carboxyl-terminal portion of the ε1 and ε2 subunits. DNA fragments that encode the amino acid residues 1335–1414 of the ε1 subunit (Meguro et al., 1992) or the amino acid residues 1353–1432 of the ε2 subunit (Kutsuwada et al., 1992) were amplified by PCR using appropriate synthetic oligonucleotides and were cloned into the expression vector pGEX-2T (Smith and Johnson, 1988) for production of the fusion proteins with glutathione S-transferase. The expression plasmids were transformed into *Escherichia coli* BL21. Induction and purification of the fusion proteins were performed as described (Araki et al., 1993). The fusion proteins were purified further by SDS-PAGE and were used for immunizing New Zealand white rabbits.

The ε1 mutant (−/−) and wild-type (+/+) mice of various postnatal ages were decapitated under anesthesia, and cerebella were removed rapidly. Each cerebellum was homogenized in 10 vol of buffer H (10 mM Tris-Cl, pH7.2, 5 mM EDTA, 0.32 M sucrose, 1 mM phenylmethylsulfonyl fluoride, and 10 mg/l leupeptin) within 3 min of decapitation, and centrifuged at 700 × *g* for 10 min to obtain a postnuclear fraction. Protein determinations were made by the method of Lowry et al. (1951). Various amounts of the protein prepared at different postnatal ages were fractionated by SDS-PAGE to ensure that densitometric measurements were within the linear range. The proteins in the gel were electroblotted onto a nitrocellulose membrane (Schleicher and Schuell, Dassel, Germany). The blots were immunoreacted with anti-ε1 and anti-ε2 sera at a dilution of 1:800 and 1:1600, respectively, and were visualized by chemiluminescence (ECL detection system, Amersham, Tokyo, Japan). For quantitative analysis, the immunoreactive bands were scanned using a computing densitometer (Shimazu CS-9300PC).

RESULTS

Developmental changes in NMDAR single-channel currents and ε2 subunit protein

Single-channel currents were induced by NMDA applied to outside-out patches excised from granule cells in cerebellar slices (Fig. 1). In wild-type (+/+) mice at postnatal day 9 (P9), the channel openings were predominantly of the high-conductance class (Stern et al., 1992; Farrant et al., 1994; Cull-Candy et al., 1995) with a main conductance of 49.2 ± 1.1 pS and a subconductance of 40.2 ± 1.1 pS in the presence of 1 mM Ca^{2+} ($n = 5$ patches). Transitions between the two levels were observed frequently (Fig. 1*A*). As animals matured, another class of NMDAR channels with lower conductance levels appeared in addition to the high-conductance channels (Fig. 1*B*). At P21, 27% of all channel openings observed were of this low-conductance type (Fig. 2*A*, *open circle*) with main and subconductance levels of 36.4 ± 0.64 pS and 19.5 ± 1.7 pS, respectively ($n = 4$). Within each conductance class, direct transitions were observed clearly between the main level and sublevel. However, no transitions were observed between high- and low-conductance events, suggesting that the two distinct classes of channel openings arise from two different receptor types, which can coexist in a patch. These results in wild-type mice are in good agreement with those obtained in normal rat cerebellar granule cells (Farrant et al., 1994).

Next, we recorded the NMDAR single-channel currents from cerebellar granule cells of mutant mice with their ε1 subunit ablated by gene knock-out techniques (Sakimura et al., 1995). In homozygous ε1-ablated (−/−) mice at the early postnatal period (P9), the NMDAR channel conductance profile was indistinguishable from that of wild-type (+/+) mice, with a main conductance of 50.0 ± 0.60 pS and a subconductance of 40.3 ± 0.59 pS ($n = 7$) (Fig. 1*C*). However, at P21, this high-conductance class became less frequent (15%) (Fig. 2*A*), and the low-conductance channels with a main conductance of 33.7 ± 1.4 pS and a subconductance of 18.2 ± 0.52 pS ($n = 6$) became dominant (Fig. 1*D*). At P30, high-conductance channels were virtually absent (<1%), leaving only low-conductance channels (Fig. 2*A*). These results suggest a progressive change during development from the expression of high-conductance channels to the expression of low-conductance channels.

The decline in expression of high-conductance channels during development of ε1 mutant (−/−) mice contrasts with their continuous presence in wild-type mice. This suggests that the ε1 subunit normally forms high-conductance channels, presumably with the ζ1 subunit as it does for recombinant NMDARs (Stern et al., 1992). Recombinant NMDARs composed of NR2B (ε2) and NR1 (ζ1) likewise form high-conductance channels (~50/40 pS), whereas those of NR2C (ε3) and NR1 (ζ1) form low-conductance channels (~36/19 pS) (Stern et al., 1992). *In situ* hybridization studies in cerebellar granule cells indicate that the ε2 subunit mRNA is present only in the first and second postnatal weeks and disappears thereafter, whereas mRNAs encoding the ε1 or ε3 subunit appear relatively late and persist in the adult (Watanabe et al., 1992, 1994; Akazawa et al., 1994; Monyer et al., 1994). Our results with native NMDARs, taken together with these reports on recombinant NMDARs, suggest that an ε2-to-ε3 subunit switch underlies the developmental shift of the NMDAR channel

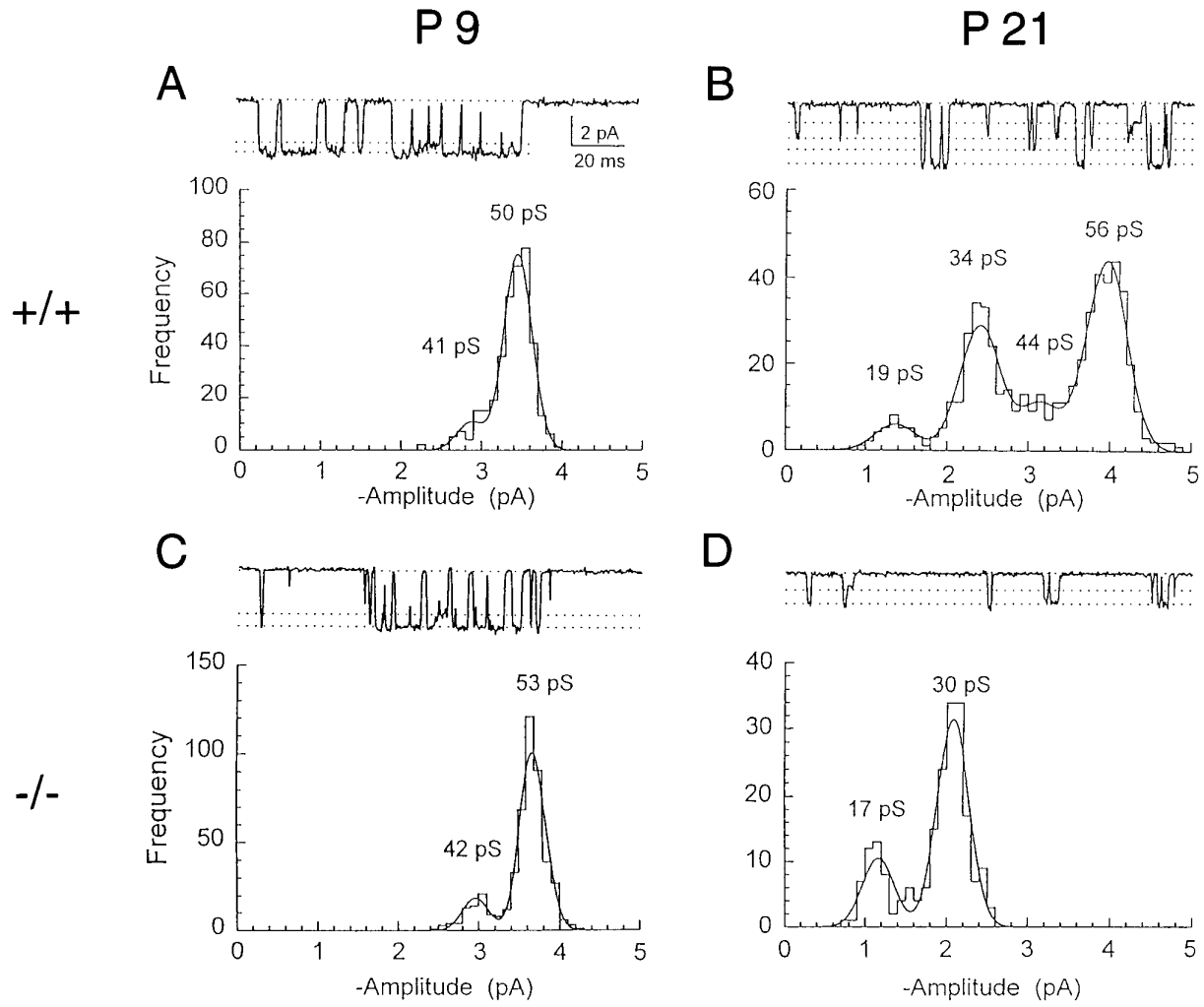

Figure 1. NMDA-gated single-channel currents in outside-out patches excised from cerebellar granule cells of wild-type and ϵ1 subunit-ablated mutant mice. Single-channel currents were activated by 50 μM NMDA in patches excised from cerebellar granule cells at −70 mV holding potential in nominally Mg^{2+}-free solution containing 1 mM Ca^{2+}, 10 μM glycine, 0.3 μM tetrodotoxin, and 1.0 μM strychnine. Channel openings in a patch from P9 (*A*) and P21 (*B*) wild-type (+/+) mice and P9 (*C*) and P21 (*D*) ϵ1 mutant (−/−) mice are shown. In *D*, the currents recorded from the patch with only low-conductance channels are illustrated. *Dashed lines* in sample records (*upper panel*) indicate the mean current amplitudes derived from the corresponding single-channel amplitude distribution (histograms in *lower panels*). Main levels and sublevels of high-conductance channels were 49.2 ± 1.1 pS and 40.2 ± 1.1 pS (n = 5) at P9 wild-type, 51.8 ± 1.4 pS and 42.3 ± 2.1 pS (n = 6) at P21 wild-type, and 50.0 ± 0.60 pS and 40.3 ± 0.59 pS (n = 7) at P9 ϵ1 mutant (−/−). Main levels and sublevels of low-conductance channels were 36.4 ± 0.64 and 19.5 ± 1.7 pS (n = 4) at P21 wild-type and 33.7 ± 1.4 pS and 18.2 ± 0.52 pS (n = 6) at P21 ϵ1 mutant (−/−). For illustration, records were filtered at 1 kHz (−3 dB).

population from the high-conductance class to the low-conductance class in ϵ1-ablated mutant mice.

The age-dependent reduction in the ϵ2 subunit protein level was determined using Western blot analysis of whole cerebellar tissue. Because NMDARs appear to be expressed exclusively in neurons (Wyllie et al., 1991) and the granule cell is the most abundant neuron in the cerebellum, these measurements should reflect subunit expression by granule cells. As illustrated in the inset of Figure 2*B*, the density of the ϵ2 subunit protein decreased with postnatal development in both wild-type (+/+, *lower panel*) and ϵ1 mutant (−/−, *upper panel*) mice. The relative amount of the ϵ2 subunit protein was quantified densitometrically at different postnatal periods (Fig. 2*B*). In developing ϵ1 mutant (−/−) mice, the time course of decline in cerebellar ϵ2 subunit protein (Fig. 2*B*, *filled circles*) was strikingly similar to that of the loss of high-conductance channels in granule cell patches (Fig. 2*A*). The decline of the ϵ2 subunit protein in wild-type cerebellum (+/+, *open circles* in Fig. 2*B*) was essentially the same as that in the ϵ1 mutant (−/−, *filled circles*), suggesting that the disruption of the ϵ1 subunit gene had no effect on the expression of the ϵ2 subunit. The ϵ2 subunit protein persisted until 1 postnatal month, although its mRNA was no longer detectable after 2 postnatal weeks (Watanabe et al., 1992, 1994).

Developmental changes in the NMDA receptor-mediated EPSCs

Next, we examined which ϵ subunits contribute to excitatory synaptic transmission at cerebellar mossy fiber–granule cell synapses. Stimulation of mossy fibers in the white matter evoked EPSCs in granule cells in both wild-type and ϵ1 mutant (−/−) mice. Application of CNQX (20 μM) blocked a fast AMPA-receptor-mediated component of the EPSC, leaving a slow NMDAR-mediated component (NMDA-EPSC) that was blocked by the NMDAR antagonists D-2-amino-5-phosphonopentanoic

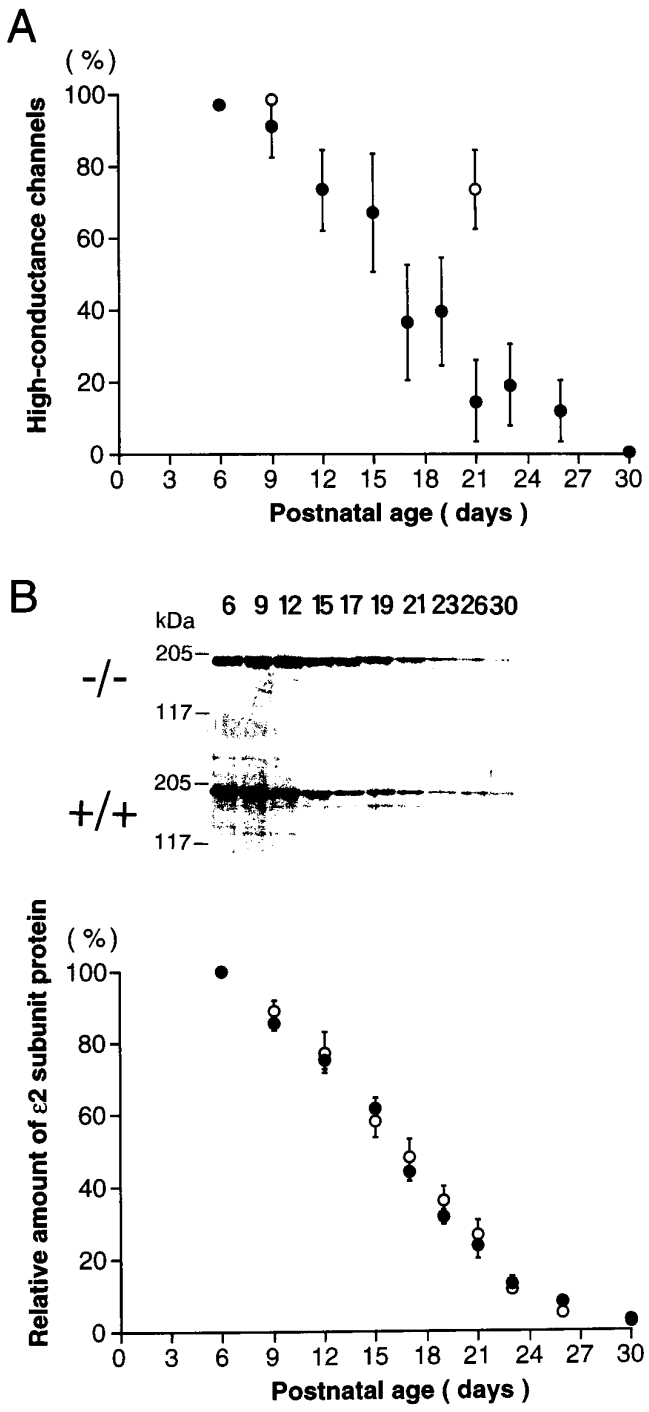

Figure 2. Developmental declines in high-conductance channels in ε1 mutant (−/−) mice and ε2 subunit protein in mutant and wild-type mice. *A*, The proportion of high-conductance (~50/40 pS) NMDAR channels in cerebellar granule cells plotted against postnatal age. *Filled circles* are data from ε1 mutant (−/−) mice. *Open circles* are those from wild-type mice. The fraction of high-conductance channel events of all openings in a patch was measured from an event histogram (Fig. 1), and the mean value of four to eight patches (*symbols*) and SEM (*bars*) were indicated at each period. *B*, Relative amount of immunoreactive ε2 subunit in whole cerebella of ε1 mutant (*filled symbols*) and wild-type (*open symbols*) mice at various postnatal days. Individual values were determined by densitometric measurements of immunoreactive bands shown in the *inset* and were normalized to the value at P6. There was no difference in the amount of ε2 subunit protein between wild-type and mutant mice at P6. Each data point derived from five to nine mice cerebella. *Inset*, 50 μg each of postnuclear proteins of cerebella of ε1 mutant mice (−/−, *upper panel*) and wild-type (+/+, *lower panel*) mice was loaded on each lane of SDS-PAGE (7% gel). After electrophoresis, the protein was electrotransferred onto a nitrocellulose membrane. The blot then was probed with antiserum (1:1600) against ε2, and protein bands were visualized by a chemiluminescence detection system (Amersham). Molecular mass markers are indicated on the *left*, and age of animals are indicated on *top*. Western blot analyses of proteins from ε1 mutant (−/−) mice using anti-ε1 antibodies revealed no detectable immunoreactive bands, whereas the levels of the ε1 subunit protein increased during the postnatal development in wild-type mice (data not shown).

acid (100 μM) and 7-chlorokynurenic acid (40 μM). NMDA-EPSCs were first observed at ~P5 and could be consistently evoked after P7 (Fig. 3*A*). As animals matured, NMDA-EPSCs appeared to become smaller. In Mg^{2+}-free solution at −70 mV, the mean amplitude of the NMDA-EPSCs evoked by a supramaximal stimulus intensity was 77.6 ± 12 pA (n = 20) at P7–P9, whereas it was 21.2 ± 1.6 pA at P21–P24 (n = 30) in wild-type mice. Similarly in ε1 mutant (−/−) mice, the amplitude of NMDA-EPSCs was 73.9 ± 9.7 pA (n = 22) at P7–P9, but only 18.5 ± 2.3 pA (n = 20) at P21–P24 (Fig. 3*A*).

Kinetic properties

In both wild-type and mutant mice, the decay time course of NMDA-EPSCs could be well described by a double exponential function. In the wild-type mice, the time constants for the fast and slow components were 51.8 ± 4.8 msec (57.3 ± 3.0%) and 377 ± 37 msec at P7–P9 (n = 20), and 35.7 ± 1.6 msec (76.8 ± 1.5%) and 254 ± 24 msec at P21–P24 (n = 30). Thus during development, there was a clear acceleration in the EPSC decay, with a significant decrease of both fast and slow time constants as well as an increase in the relative amplitude of the fast component ($p < 0.01$, Student's t test). A similar developmental change also was seen in the mutant mice, for which the corresponding values were 87.8 ± 6.0 msec (48.2 ± 3.2%) and 471 ± 65 msec at P7–P9 (n = 22), and 44.2 ± 3.4 msec (59.0 ± 2.5%) and 227 ± 15 msec at P21–P24 (n = 20). However, deletion of the ε1 subunit from synaptic NMDARs clearly resulted in a slowing of the fast component decay and a decrease in its relative amplitude in both P7–P9 and P21–P24 mutant mice ($p < 0.02$). This is illustrated in Figure 3*B* as a plot of NMDA-EPSC rise time (10–90%) against decay time (from peak to 37%) at P21–P24. Between wild-type and ε1 mutant (−/−) mice, a clear difference was observed in decay time, with the former (47.0 ± 2.1 msec, n = 30) being significantly shorter than the latter (74.2 ± 2.5 msec, n = 20, $p < 0.0001$), whereas no difference was observed in NMDA-EPSC rise time between the groups at P21–P24 (wild-type 7.91 ± 0.45 msec; mutant 7.72 ± 0.38 msec). Similarly at P7–P9, the NMDA-EPSC decay time of wild-type mice (102 ± 5.5 msec, n = 20) was significantly faster than that of mutant mice (169 ± 8.5 msec, n = 22, $p < 0.0001$).

Voltage-dependent Mg^{2+} block

One important feature of NMDAR channels is their sensitivity to voltage-dependent block by Mg^{2+} (Nowak et al., 1984). Current–voltage relationships were obtained for the NMDA-EPSCs at early (P7–P9) and late (P21–P24) postnatal periods in wild-type (+/+) and ε1 mutant (−/−) mice (Fig. 4). At P7–P9, NMDA-EPSCs in both wild-type and ε1 mutant (−/−) mice showed a typical voltage-dependent block by 0.1 mM Mg^{2+} (*left panels* in Fig. 4*A*,*B*; *filled circles* in *B*), with the amplitude being smaller at more negative potentials. As expected, the block was more pronounced in 1 mM Mg^{2+} (*open circles* in Fig. 4*B*). At P21–P24, the

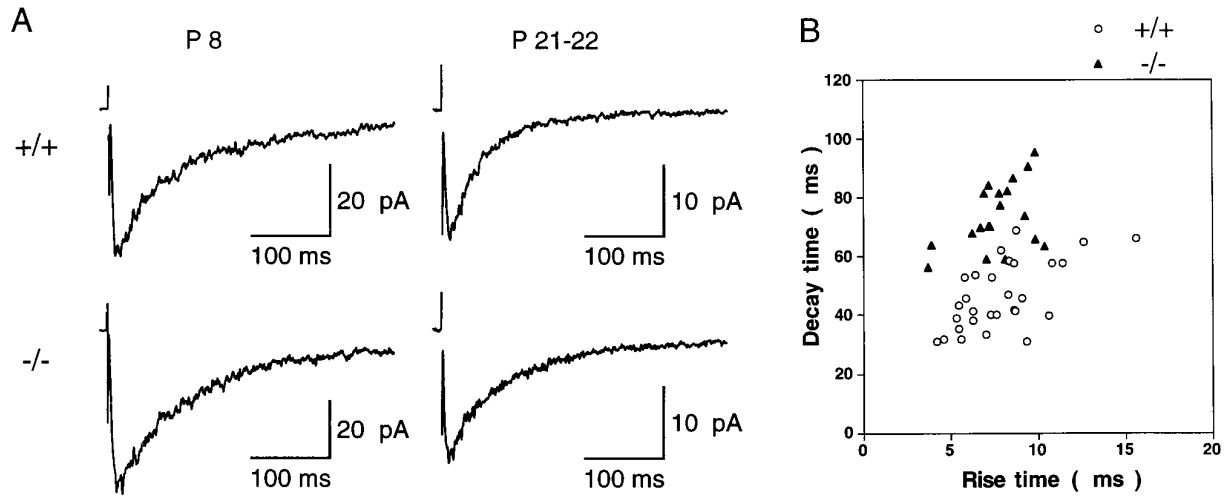

Figure 3. NMDA-EPSCs evoked in cerebellar granule cells by stimulating mossy fiber inputs. *A*, Averaged NMDA-EPSCs recorded from cerebellar granule cells of wild-type (+/+, *upper row*) and ε1 mutant mice (−/−, *lower row*) at early (*P8*, *left column*) and late (*P21–P22*, *right column*) postnatal stages. In Mg^{2+}-free solution containing CNQX (20 μM), bicuculline (10 μM), and strychnine (0.5 μM). EPSCs (20–25) were averaged for each trace. Holding potential was −70 mV. *B*, A kinetic comparison of NMDA-EPSCs. Rise time (10–90%, *abscissa*) and decay time (from peak to 37%, *ordinate*) were compared between wild-type (*open circles*) and ε1 mutant (−/−) mice (*filled triangles*) at P21–P24.

degree of Mg^{2+} block was reduced in both wild-type and ε1 mutant (−/−) mice (*right panels* in Fig. 4*A*,*B*). At a holding potential of −70 mV, the peak amplitude of NMDA-EPSCs remaining in 0.1 mM Mg^{2+} (Fig. 5*A*) in wild-type mice (*open column*) at P7–P9 was 26 ± 3.9% of that in Mg^{2+}-free solution ($n = 6$), whereas it was 65 ± 4.4% at P21–P24 ($n = 6$) (significant difference at $p < 0.0001$). Similarly in ε1 mutant (−/−) (*filled columns*), the remaining proportion of NMDA-EPSCs in 0.1 mM Mg^{2+} was significantly smaller at the early period than at the late period (19 ± 3.4%, $n = 6$ vs 61 ± 7.1%, $n = 5$) ($p < 0.001$). Also in 1 mM Mg^{2+} (Fig. 5*B*) in both wild-type and mutant, the proportion of NMDA-EPSCs remaining unblocked at P21–P24 (wild-type, 15 ± 2.6%, $n = 5$; mutant, 21 ± 2.0%, $n = 5$) was larger than that at P7–P9 (wild-type, 5.3 ± 0.99%, $n = 5$; mutant, 4.1 ± 0.68%, $n = 7$) (these values are significantly different: $p < 0.01$ in the wild-type and $p < 0.0001$ in the mutant). Thus, the extent of Mg^{2+} block of NMDA-EPSCs *decreased* in an age-dependent manner but was independent of the presence of the ε1 subunit.

DISCUSSION

Comparison of native and recombinant NMDAR channel properties

We observed a clear change in the NMDA receptor channel properties in developing cerebellar granule cells. In wild-type mice, high-conductance channel openings (~50/40 pS) were observed at high frequency over the entire postnatal period examined (P7–P29), whereas in ε1 mutant (−/−) mice, these were observed only at an early postnatal stage. Low-conductance channel openings (~35/20 pS) appeared in both wild-type and ε1 mutant (−/−) mice only at a late stage. *In situ* hybridization studies indicate that mRNAs encoding the ε1 or ε3 subunit are expressed relatively late postnatally, whereas the ε2 subunit mRNAs appear transiently during early postnatal development (Watanabe et al., 1992; 1994; Akazawa et al., 1994; Monyer et al., 1994). The ε2 subunit protein in cerebellar tissue examined by Western blot analysis displayed an age-dependent decline that was similar in time course to the decline in the proportion of high-conductance channels in cerebellar granule cells of ε1 mutant (−/−) mice. Thus, the channel conductances observed in native cerebellar tissue correspond well with those reported for recombinant NMDARs containing the ζ1 subunit in combination with one of the ε subunits; high-conductance channels are formed by the ζ1 (NR1) subunit in combination with either ε1 (NR2A) or ε2 (NR2B) subunit, whereas low-conductance channels are composed of the ζ1 (NR1) subunit together with the ε3 (NR2C) subunit (Stern et al., 1992; Cull-Candy et al., 1995). Our present results support the hypothesis that different ε subunits in combination with the ζ1 subunit form distinct NMDARs in cerebellar granule cells, although we cannot exclude the possibilities that multiple ε subunits including those undiscovered may contribute to individual NMDARs *in situ* (Sheng et al., 1994).

Synaptic currents mediated by NMDARs

NMDA-EPSCs were recorded from cerebellar granule cells of ε1 mutant (−/−) mice at early or late postnatal stages when the ε2 or ε3 subunit, respectively, is predominantly expressed. Comparison of wild-type and mutant NMDA-EPSCs indicated that expression of the ε1 subunit resulted in a faster decay time of NMDA-EPSCs. Therefore, distinct ε subunits appear to be expressed subsynaptically and contribute to excitatory synaptic transmission at different stages of development.

The decay time of the NMDA-EPSCs is known to be much longer than the mean open time or burst length of NMDAR channels (Edmonds and Colquhoun, 1992; Lester and Jahr, 1992), but it is comparable to the deactivation time of NMDAR current responses in patches (Lester et al., 1990; Lester and Jahr, 1992), possibly because of a prolonged latency to first opening (Edmonds and Colquhoun, 1992). The deactivation time of NMDAR current responses is faster for agonists of low affinity (Lester and Jahr, 1992). Recombinant ε1–ζ1 (NR2A–NR1) NMDARs have the lowest affinity for L-glutamate (Kutsuwada et al., 1992; Ishii et al., 1993) and the fastest current deactivation time (Monyer et al., 1994). Consistent with this observation, our present results indicate that ε1 subunit ablation slows the decay time of NMDA-EPSCs. In contrast to the ε2 subunit, expression of the ε1 subunit

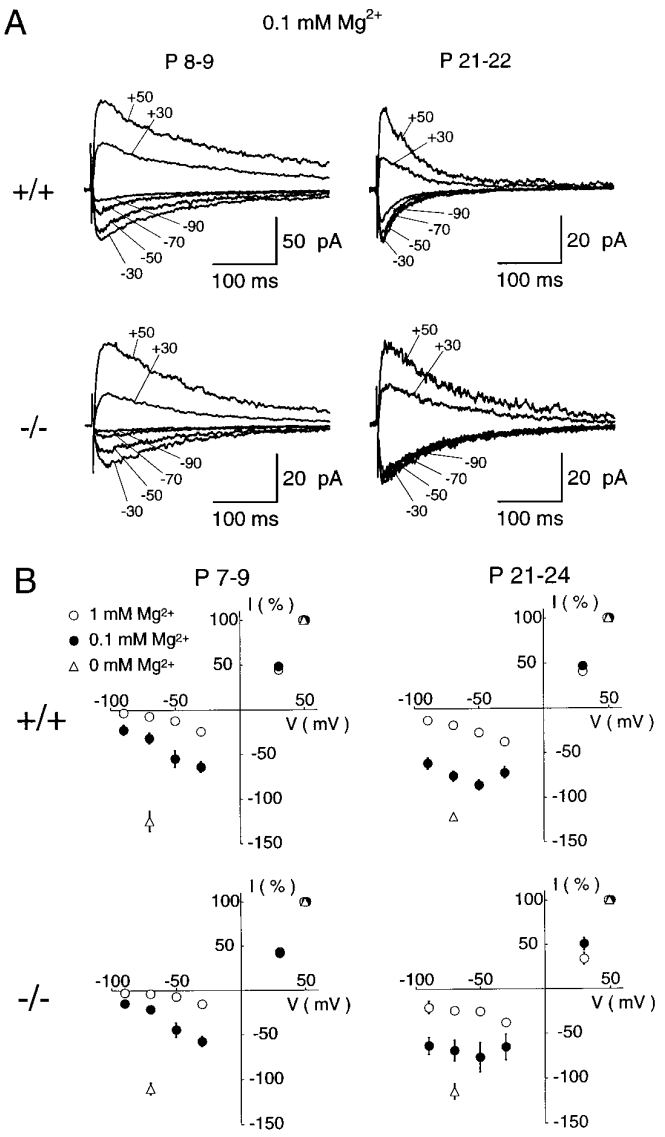

Figure 4. Voltage-dependent Mg^{2+} block of NMDA-EPSCs. *A*, NMDA-EPSCs recorded in the presence of 0.1 mM Mg^{2+} at different holding potentials are superimposed. Records are from cerebellar granule cells of wild-type mice at P8 (*top left*) and P21 (*top right*), and ϵ1 mutant (−/−) mice at P9 (*bottom left*) and P22 (*bottom right*) periods. Each trace is averaged from 12 to 20 EPSCs. *B*, Current–voltage (*I–V*) relationships of NMDA-EPSCs from wild-type mice (*top panels*) and ϵ1 mutant (−/−) mice (*bottom panels*) at the early (*left panels*) and late (*right panels*) postnatal periods. Data points are obtained in the presence of 0.1 mM Mg^{2+} (*filled circles*) or 1 mM Mg^{2+} (*open circles*), or in the nominal absence of external Mg^{2+} (*open triangles* at −70 mV). The EPSC amplitudes were normalized to the mean value at + 50 mV in each experimental condition. Each data point and error bar indicates mean and SEM of NMDA-EPSCs derived from 5 to 11 cells.

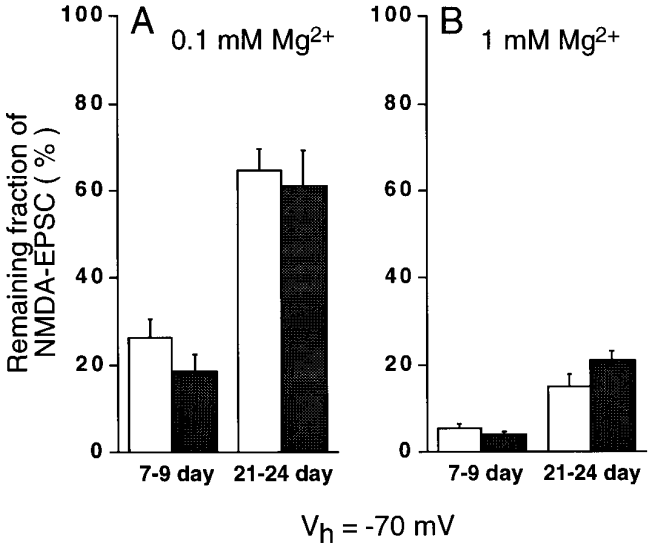

Figure 5. Mg^{2+} block of NMDA-EPSCs at −70 mV. Amplitude of NMDA-EPSCs remaining after Mg^{2+} block relative to those in Mg^{2+} -free solution in wild-type (*open column*) and ϵ1 mutant (−/−) (*filled column*) mice. Extracellular Mg^{2+} concentration was 0.1 mM (*A*) and 1 mM (*B*), respectively. Significant difference was found for the remaining EPSCs between P7–P9 and P21–P24 in wild-type mice (*between filled columns* in *A*) ($p < 0.0001$) and mutant mice (*between open columns* in *A*) ($p < 0.001$) in 0.1 mM Mg^{2+}, as well as in 1 mM Mg^{2+} (*B*) ($p < 0.01$ and $p < 0.0001$ for wild-type and mutant mice, respectively). The difference in the remaining EPSCs was not significant between wild-type and mutant in 0.1 mM Mg^{2+} or in 1 mM Mg^{2+}. The mean amplitude of NMDA-EPSCs remaining in 1 mM Mg^{2+} at −70 mV was 4.2 and 6.6 pA for wild-type and mutant mice granule cells, respectively, at P21–P24, whereas the corresponding values at P7–P9 were 2.7 and 2.0 pA, respectively.

increases with postnatal development (Watanabe et al., 1992, 1994). Therefore, the ϵ2-to-ϵ1 subunit switch may underlie developmental acceleration in the kinetics of NMDA-EPSCs at the mossy fiber–granule cell synapse. This mechanism also may underlie the kinetic changes during development reported in the superior colliculus (Hestrin, 1992) and the visual cortex (Carmignoto and Vicini, 1992) of rats, although additional factors such as developmental changes in the ζ subunit splice variants (Della Vedova et al., 1994) also could contribute. In this regard, the developmental switch from ϵ2 to ϵ1 subunit of NMDARs at the cerebellar synapses appears analogous to the γ-to-ϵ subunit switch of nicotinic acetylcholine receptors at the neuromuscular junction (Mishina et al., 1986) and the α2-to-α1 subunit switch of glycine receptors at spinal inhibitory synapses (Takahashi et al., 1992).

The voltage-dependent Mg^{2+} block of NMDAR is thought to play a crucial role in synaptic plasticity, because it can prevent Ca^{2+} entry through the receptor into cells at the resting potential. It has been reported that NMDARs in visual cortical neurons are relatively insensitive to Mg^{2+} at the early developmental period (Kato and Yoshimura, 1993). In contrast, our results demonstrate that NMDA-EPSCs in cerebellar granule cells were less sensitive to Mg^{2+} block at the later postnatal period. Because this phenomenon was observed in both wild-type and ϵ1 mutant (−/−) mice, it is most likely that the ϵ3 subunit rather than the ϵ1 subunit is responsible for this change. In fact, the recombinant NMDAR ϵ3–ζ1 (NR2C–NR1) is relatively resistant to Mg^{2+} compared with ϵ1–ζ1 (NR2A–NR1) or ϵ2–ζ1 (NR2B–NR1) receptors (Kutsuwada et al., 1992; Monyer et al., 1992). Our results from native NMDARs together with these reports on recombinant NMDARs suggest that the developmental reduction in the sensitivity of NMDARs to Mg^{2+} block is a result of the ϵ3 subunit expressed at the relatively late stage of development.

During postnatal development, NMDA-EPSCs became faster in decay time, smaller in peak amplitude, and more resistant to the voltage-dependent block by Mg^{2+}. Reductions in time course and amplitude of NMDA-EPSCs would contribute to reduced Ca^{2+} entry through NMDARs during synaptic transmission, whereas a decrease in Mg^{2+} block would increase the Ca^{2+} entry

particularly at the resting membrane potential. NMDARs also are present on premigratory and migrating granule cells before synapse formation (Farrant et al., 1994), and Ca^{2+} entry through these receptors appears to contribute to cell migration (Komuro and Rakic, 1993). The precise role of synaptic NMDAR-mediated Ca^{2+} entry into postmigratory granule cells remains to be elucidated.

REFERENCES

Akazawa C, Shigemoto R, Bessho Y, Nakanishi S, Mizuno N (1994) Differential expression of five *N*-methyl-D-aspartate receptor subunit mRNAs in the cerebellum of developing and adult rats. J Comp Neurol 347:150–160.

Araki K, Meguro H, Kushiya E, Takayama C, Inoue Y, Mishina M (1993) Selective expression of the glutamate receptor channel δ2 subunit in cerebellar Purkinje cells. Biochem Biophys Res Commun 197:1267–1276.

Blanton MG, Turco JJL, Kriegstein AR (1989) Whole cell recording from neurons in slices of reptilian and mammalian cerebral cortex. J Neurosci Methods 30:203–210.

Carmignoto G, Vicini S (1992) Activity-dependent decrease in NMDA receptor responses during development of the visual cortex. Science 258:1007–1011.

Colquhoun D, Sigworth FJ (1995) Fitting and statistical analysis of single-channel records. In: Single-channel recording, 2nd ed (Sakmann B, Neher E, eds), pp 483–587. New York: Plenum.

Cull-Candy SG, Farrant M, Feldmeyer D (1995) NMDA channel conductance: a user's guide. In: Excitatory amino acids and synaptic function, 2nd ed (Wheal H, Thompson AM, eds) pp 121–132. New York: Academic.

D'Angelo E, Rossi P, Taglietti V (1993) Different proportions of *N*-methyl-D-aspartate and non-*N*-methyl-D-aspartate receptor currents at the mossy fibre-granule cell synapse of developing rat cerebellum. Neuroscience 53:121–130.

Della Vedova F, Bonecchi L, Bianchetti A, Fariello RG, Speciale C (1994) Age-related changes in the relative abundance of NMDAR1 mRNA spliced variants in the rat brain. NeuroReport 5:581–584.

Edmonds B, Colquhoun D (1992) Rapid decay of averaged single-channel NMDA receptor activations recorded at low agonist concentration. Proc R Soc Lond [Biol] 250:279–286.

Edwards FA, Konnerth A, Sakmann B, Takahashi T (1989) A thin slice preparation for patch clamp recordings from neurones of the mammalian central nervous system. Pflügers Arch 414:600–612.

Farrant M, Feldmeyer D, Takahashi T, Cull-Candy SG (1994) NMDA-receptor channel diversity in the developing cerebellum. Nature 368:335–339.

Garthwaite J, Brodbelt AR (1989) Synaptic activation of *N*-methyl-D-aspartate and non-*N*-methyl-D-aspartate receptors in the mossy fibre pathway in adult and immature rat cerebellar slices. Neuroscience 29:401–412.

Hestrin S (1992) Developmental regulation of NMDA receptor-mediated synaptic currents at a central synapse. Nature 357:686–689.

Ikeda K, Nagasawa M, Mori H, Araki K, Sakimura K, Watanabe M, Inoue Y, Mishina M (1992) Cloning and expression of the ϵ4 subunit of the NMDA receptor channel. FEBS Lett 313:34–38.

Ishii T, Moriyoshi K, Sugihara H, Sakurada K, Kadotani H, Yokoi M, Akazawa C, Shigemoto R, Mizuno M, Masu M, Nakanishi S (1993) Molecular characterization of the family of the *N*-methyl-D-aspartate receptor subunits. J Biol Chem 268:2836–2843.

Kato N, Yoshimura H (1993) Reduced Mg^{2+} block of *N*-methyl-D-aspartate receptor-mediated synaptic potentials in developing visual cortex. Proc Natl Acad Sci USA 90:7114–7118.

Komuro H, Rakic P (1993) Modulation of neuronal migration by NMDA receptors. Science 260:95–97.

Kutsuwada T, Kashiwabuchi N, Mori H, Sakimura K, Kushiya E, Araki K, Meguro H, Masaki H, Kumanishi T, Arakawa M, Mishina M (1992) Molecular diversity of the NMDA receptor channel. Nature 358:36–41.

Lester RAJ, Jahr CE (1992) NMDA channel behavior depends on agonist affinity. J Neurosci 12:635–643.

Lester RAJ, Clements JD, Westbrook GL, Jahr CE (1990) Channel kinetics determine the time course of NMDA receptor-mediated synaptic currents. Nature 346:565–567.

Lowry OH, Rosebrough NJ, Farr AL, Randall RJ (1951) Protein measurement with the folin phenol reagent. J Biol Chem 193:265–275.

Meguro H, Mori H, Araki K, Kushiya E, Kutsuwada T, Yamazaki M, Kumanishi T, Arakawa M, Sakimura K, Mishina M (1992) Functional characterization of a heteromeric NMDA receptor channel expressed from cloned cDNAs. Nature 357:70–74.

Mishina M, Takai T, Imoto K, Noda M, Takahashi T, Numa S, Methfessel C, Sakmann B (1986) Molecular distinction between fetal and adult forms of muscle acetylcholine receptor. Nature 321:406–411.

Monyer H, Sprengel R, Schoepfer R, Herb A, Higuchi M, Lomeli H, Burnashev N, Sakmann B, Seeburg PH (1992) Heteromeric NMDA receptors: molecular and functional distinction of subtypes. Science 256:1217–1221.

Monyer H, Burnashev N, Laurie DJ, Sakmann B, Seeburg PH (1994) Developmental and regional expression in the rat brain and functional properties of four NMDA receptors. Neuron 12:529–540.

Moriyoshi K, Masu M, Ishii T, Shigemoto R, Mizuno N, Nakanishi S (1991) Molecular cloning and characterization of the rat NMDA receptor. Nature 354:31–37.

Nowak L, Bregestovski P, Ascher P, Herbet A, Prochiantz A (1984) Magnesium gates glutamate-activated channels in mouse central neurones. Nature 307:462–465.

Rabacchi S, Bailly Y, Delhaye-Bouchaud N, Mariani J (1992) Involvement of the *N*-methyl-D-aspartate (NMDA) receptor in synapse elimination during cerebellar development. Science 256:1823–1825.

Sakimura K, Kutsuwada T, Ito I, Manabe T, Takayama C, Kushiya E, Yagi T, Aizawa S, Inoue Y, Sugiyama H, Mishina M (1995) Reduced hippocampal LTP and spatial learning in mice lacking NMDA receptor ϵ1 subunit. Nature 373:151–155.

Sheng M, Cummings J, Roldan LA, Jan YN, Jan LY (1994) Changing subunit composition of heteromeric NMDA receptors during development of rat cortex. Nature 368:144–147.

Silver RA, Traynelis SF, Cull-Candy SG (1992) Rapid-time-course miniature and evoked excitatory currents at cerebellar synapses *in situ*. Nature 355:163–166.

Smith DB, Johnson KS (1988) Single-step purification of polypeptides expressed in *Escherichia coli* as fusions with glutathione S-transferase. Gene 67:31–40.

Stern P, Béhé P, Schoepfer R, Colquhoun D (1992) Single-channel conductances of NMDA receptors expressed from cloned cDNAs: comparison with native receptors. Proc R Soc Lond [Biol] 250:271–277.

Takahashi T, Momiyama A, Hirai K, Hishinuma F, Akagi H (1992) Functional correlation of fetal and adult forms of glycine receptors with developmental changes in inhibitory synaptic receptor channels. Neuron 9:1155–1161.

Tsuzuki K, Mochizuki S, Iino M, Mori H, Mishina M, Ozawa S (1994) Ion permeation properties of the cloned mouse ϵ2/ζ1 NMDA receptor channel. Mol Brain Res 26:37–46.

Watanabe M, Inoue Y, Sakimura K, Mishina M (1992) Developmental changes in distribution of NMDA receptor channel subunit mRNAs. NeuroReport 3:1138–1140.

Watanabe M, Mishina M, Inoue Y (1994) Distinct spatiotemporal expressions of five NMDA receptor channel subunit mRNAs in the cerebellum. J Comp Neurol 343:513–519.

Wyllie DJA, Mathie A, Symonds CJ, Cull-Candy SG (1991) Activation of glutamate receptors and glutamate uptake in identified microglial cells in rat cerebellar cultures. J Physiol (Lond) 432:235–258.

Yamazaki M, Mori H, Araki K, Mori KJ, Mishina M (1992) Cloning, expression and modulation of a mouse NMDA receptor subunit. FEBS Lett 300:39–45.